Optimizing the Cost and Reliability of Shared Anchors in an Array of Floating Offshore Wind Turbines

Michael C. Devin
School of Mechanical, Industrial, and Manufacturing Engineering,
Oregon State University,
Corvallis, OR 97331

Bryony L. DuPont[1]
School of Mechanical, Industrial, and Manufacturing Engineering,
Oregon State University,
Corvallis, OR 97331
e-mail: bryony.dupont@oregonstate.edu

Spencer T. Hallowell
Baker Design Consultants,
Freeport, ME 04032

Sanjay R. Arwade
University of Massachusetts Amherst,
Amherst, MA 01003

Commercial floating offshore wind projects are expected to emerge in the U.S. by the end of this decade. Currently, however, high costs for the technology limit its commercial viability, and a lack of data regarding system reliability heightens project risk. This work presents an optimization algorithm to examine the tradeoffs between cost and reliability for a floating offshore wind array that uses shared anchoring. Combining a multivariable genetic algorithm with elements of Bayesian optimization, the optimization algorithm selectively increases anchor strengths to minimize the added costs of failure for a large floating wind farm in the Gulf of Maine under survival load conditions. The algorithm uses an evaluation function that computes the probability of mooring system failure, then calculates the expected maintenance costs of a failure via a Monte Carlo method. A cost sensitivity analysis is also performed to compare results for a range of maintenance cost profiles. The results indicate that virtually all of the farm's anchors are strengthened in the minimum cost solution. Anchor strength is increased between 5 and 35% depending on farm location, with anchor strength nearest the export cable being increased the most. The optimal solutions maintain a failure probability of 1.25%, demonstrating the tradeoff point between cost and reliability. System reliability was found to be particularly sensitive to changes in turbine costs and downtime, suggesting further research into floating offshore wind turbine failure modes in extreme loading conditions could be particularly impactful in reducing project uncertainty. [DOI: 10.1115/1.4051163]

1 Introduction

The U.S. is beginning to adopt offshore wind power to meet state policy goals amid increasing national power demand. Seven states on the Eastern seaboard have now cumulatively committed to nearly 20 GW of offshore wind installations by 2035 [1]. Investment is also emerging for floating offshore wind projects on the West Coast, Maine, and Hawaii. The Bureau of Ocean Energy Management has established 13 call areas in U.S. federal waters, including three off the coast of California and two near the Hawaiian island of Oahu [1]. The University of Maine recently partnered with diamond offshore wind and RWE Renewables to install a full-scale floating wind demonstration project off the coast of Maine, with completion expected in 2023 [2].

Floating offshore wind turbines (FOWTs) have shown to be viable in existing demonstration projects, and the first commercial scale FOWT installation off the Scottish coast has, at time of writing, exceeded production estimates [3]. However, floating offshore wind is currently too expensive to achieve widespread commercial viability. As of 2018, the levelized cost of energy (LCOE) of floating offshore wind is estimated at $132/MWh, far higher than the $42/MWh estimated for onshore wind [4].

Additionally, uncertainty is high regarding the reliability of commercial development of FOWTs in the United States. The metocean climate of North American waters is more severe than seen in European waters, due to harsher wave climates (for the West Coast) and the risk of hurricanes (for the Atlantic and Gulf coasts) [5]. With little historical data about FOWT behavior in these conditions, offshore wind investors for American projects endure greater project risk and uncertainty. This is compounded by experience from Europe revealing, in some cases, higher repair costs and reduced turbine lifetimes than initially expected for offshore wind projects [6].

Research in floating offshore wind is currently addressing the problems of both cost and—to a lesser but growing extent—reliability. However, these two parameters are often inversely related. For example, one proposed method to reduce costs for the mooring system is by utilizing shared anchors.[2] In a scheme designed by Fontana et al., a single suction caisson connects to three mooring lines instead of one [7]. For large wind farms, this method of sharing anchors reduces the number of anchor sites required by nearly a factor of three. This reduces overall capital costs of a system by 8–16% compared to an equivalent farm with a traditional single-line anchor system due to lowered material costs and fewer geotechnical surveys. Additionally, the symmetric loading from the three mooring lines has been found to reduce the overall force demands on an anchor by 11–16% [8]. However, sharing anchors also presents risks not present with traditional anchor systems. Hallowell et al. found the probability of failure for a given turbine in a survival load case with shared anchors increases by 12.2% compared to turbines using a traditional anchor system due to the risk of cascading failures when sharing anchors [9].

Identifying the exact relationship between cost and reliability can have major implications in project planning and system design, but has not been explored for floating offshore wind systems at time of writing. This research provides a computational method to examine the tradeoffs between reliability and costs for the anchor sharing method developed by Fontana et al. Specifically, this work presents a novel optimization method, REL-OPT [10], that selectively increases the strength of certain anchors in a large floating wind farm with shared anchors, with the goal of

[1]Corresponding author.

Manuscript received September 30, 2020; final manuscript received March 10, 2021; published online August 9, 2021. Assoc. Editor: Vikram Pakrashi.

[2]In other literature, this technology is also referring to as multiline anchoring or anchor mutualiz(s)ation.

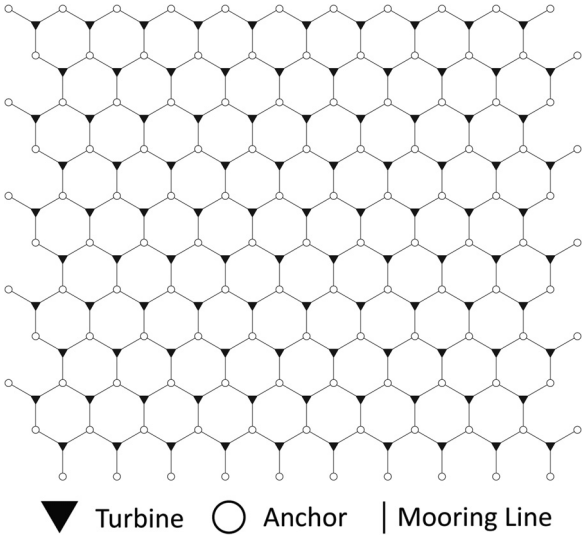

Fig. 1 Schematic of the wind farm used in this work, illustrating the anchor sharing system. Adapted from Ref. [14].

minimizing mooring system failure while balancing it with the cost of increasing anchor strength. The optimization method is a multivariable genetic algorithm modified to incorporate elements of Bayesian optimization to account for the inherent uncertainty related to failure. The evaluation function of the optimization algorithm expands on the system reliability evaluations by Hallowell et al. [9] by integrating a failure cost model. In the future, this algorithm could be adapted for other anchoring methods, which could inform strategies regarding the use of shared anchors and if the technology is cost-effective. A cost sensitivity analysis is also performed to address cost uncertainties and identify critical areas of future research for this class of problem.

2 Problem Formulation

The objective function of the optimization algorithm in this work is to minimize the added costs of a floating wind farm in survival load conditions while controlling for anchor strength. This optimization problem examines a large floating wind farm consisting of 100 turbines in a 10-by-10 array with offset rows, shown in Fig. 1. Except for perimeter anchors, each anchor moors three OC4/DeepCWind semisubmersible platforms, each platform supporting a reference National Renewable Energy Laboratory (NREL) 5-MW turbine, requiring 120 total anchors [11,12]. Wake effects are considered negligible as the turbines are greater than 10 rotor diameters apart, as per González-Longatt et al. [13]. A water depth of 200 meters is used with flat seabed bathymetry in a soft clay soil profile. This wind farm configuration is identical to that used in Hallowell et al. [9].

Additional relevant parameters of the anchor system are included in Table 1. The parameters are derived from the results of the mooring system design evaluation in Secs. 5 and 6 of Hallowell et al. [9], which uses allowable stress design methodology and upper bound plasticity methods to determine mooring line and anchor capacity, respectively. The anchor adhesion factor, underpressure, and twist misalignment are also considered in the design.

Table 1 Parameters of the analyzed floating wind farm

Overall layout	
Horizontal distance between turbines	1451 m
Radial distance from fairleads to anchors	797 m
Mooring lines	
Material	Grade R3 chains
Nominal diameter	77.9 mm
Nominal break load capacity	5111 kN
Unstretched length	835 m
Seafloor lay length	243 m
Anchors	
Nominal ultimate holding capacity	3460 kN
Angle between padeye connections	120 deg

2.1 Evaluation Function. Optimization algorithms require a clearly defined evaluation function in order to operate successfully. Discussion of the evaluation function is critical in understanding the problem the algorithm in this work aims to solve. Additionally, this helps clarify the rationale behind decisions made for other parts of the algorithm discussed in Secs. 3 and 4.

The evaluation method used in this optimization algorithm is a modification of the system reliability calculation for this shared anchor concept derived in Hallowell et al. [9]. In the work of Hallowell et al., 12 1-hour simulations of a wind turbine in a survival load case scenario are conducted in FAST, a time domain simulation software for wind turbines developed by NREL [15]. FAST simulates the nonlinear aero-hydroservo-elastic interactions of a floating wind turbine, capturing the fully coupled dynamic response of this load case. The survival load case scenario, developed by Viselli et al. [16], represents a southerly storm with a 500-year mean return period for the Gulf of Maine, which has a similar water depth and soil profile to what is being considered here. The peak tensions at various points in each mooring line and at the anchor are fit to a lognormal distribution. This distribution is randomly sampled to determine the demands on every mooring line and anchor in the wind farm. Similarly, the load capacity for each component is determined from a lognormal distribution based on the nominal load capacities in Table 1. This simulates the structural variance in mooring system components, calculated from the risk of soil degradation failure with 20% covariance as per Choi [17]. If the demand for any component exceeds its load capacity, the component fails. All turbines associated with failed components recalculate the demands on the surviving mooring lines and anchors (sampled from different distributions generated from identical FAST simulations with the respective failed mooring lines removed), again capturing any mooring system failures. This process repeats until no new failures occur. The number of turbines connected to failed components is saved, and the process repeats many times (set by the user), allowing for a reliability analysis to be performed via the Monte Carlo method. This process is visualized in Fig. 2.

The evaluation function used in this optimization algorithm (henceforth referred to as the *added cost evaluation*, visualized in Fig. 3) builds upon the work of Hallowell et al. (henceforth referred to as the *system reliability evaluation*) by adding three modifications:

(1) An additional safety factor can be specified for each anchor in the wind farm prior to the start of the evaluation. This extra safety factor is specified as a multiplier to the nominal load capacities in Table 1 prior to the lognormal sampling. The multiplier is referred to as the *overstrength factor* of an anchor for the remainder of this work. 20 discrete overstrength factors are available, ranging from 1.05 to 2.
(2) The number of Monte Carlo samples performed is now controlled by the optimization algorithm, based on the reliability and cost of the wind farm given certain overstrength factors. This is explained in greater detail in Sec. 3.2.
(3) Once the number of turbines with component failures in a given Monte Carlo simulation is determined, a cost analysis is added to calculate the costs from all applied overstrength factors and component failures. This is detailed in Sec. 4.

3 Optimization Algorithm

A custom optimization algorithm was developed for the added cost evaluation to solve this optimization problem. A

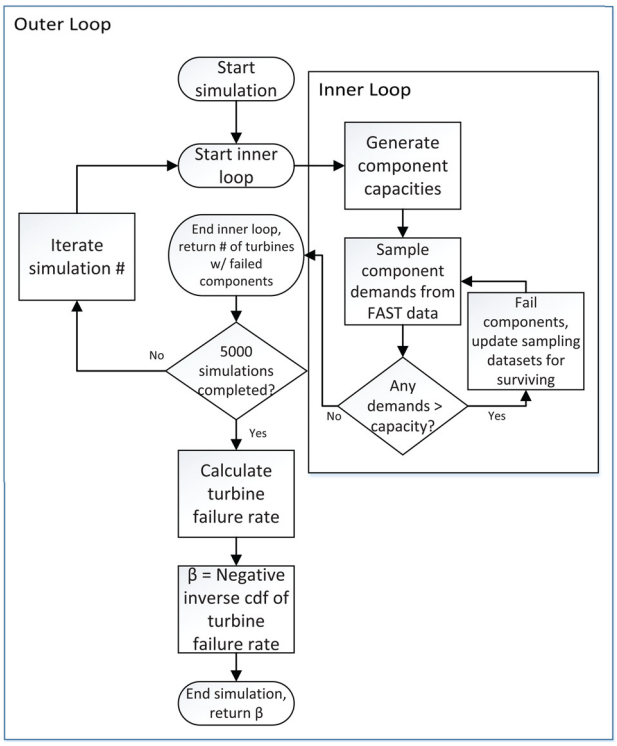

Fig. 2 System reliability evaluation used in Hallowell et al. [9]. Adapted from Ref. [14].

multivariable genetic algorithm (GA) was used as the basis for the algorithm. However, given the uncertainty present in the added cost evaluation, a GA with traditional function evaluations would output highly stochastic data, making convergence to an optimal solution challenging. This challenge is addressed by using series

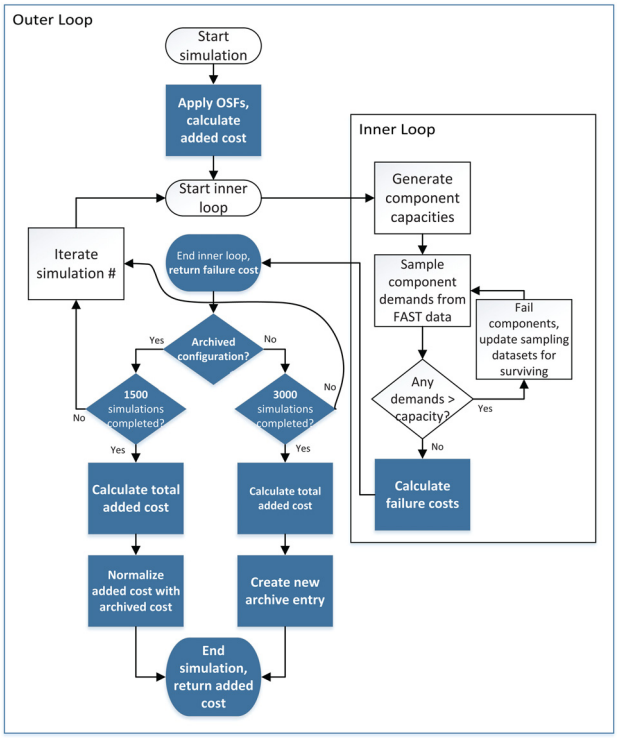

Fig. 3 Added cost evaluation process. Changes from Fig. 2 are in bold. Adapted from Ref. [14].

of function evaluations instead of a single evaluation per individual, as per Painton and Campbell [18]. This is done in this work by incorporating elements from Bayesian optimization methods to combat the stochasticity and reach convergence.

3.1 Multivariable Genetic Algorithm. Genetic algorithms are a set of heuristic optimization methods that uses principles of Darwinian natural selection to converge to a global optimum. Given a set population size, individuals are created using a random combination of the problem design variables, encoded into "bits." A function evaluates and scores each individual based on desirable heuristics. A new population is then created using the process of crossover (where two individuals from the population share their genes to create offspring) and mutation (where a segment of the bits of an offspring is altered), with more fit individuals being more likely to be selected to reproduce. Over many generations, the population gradually" evolves" to an optimal solution.

A genetic algorithm was chosen for this work for two reasons. First, this optimization problem is nondifferentiable, eliminating most classical optimization methods. Second, the problem has a large search space. This makes the problem prone to local (rather than global) convergence, which GAs can avoid more effectively than numerical optimization methods. Two-dimensional binary arrays are used to encode each individual in the GA, with each row representing a different anchor and each column indicating the selected overstrength factor for that anchor (if any). Anchor numbering begins in the southeast corner of the array and proceeds north, returning to the southern end of the next column of anchors to the west.

In order to ensure efficient convergence while avoiding local optima, the optimization algorithm was tuned extensively to strike a balance between population diversity and computational efficiency. This includes the introduction of other optional GA parameters, including elitism (where the most fit individuals are cloned directly to the next generation prior to crossover), using a kill (where the least fit individuals are ineligible from crossover to remove negative outliers), and including a set of random individuals in each population unaffected by the crossover in the previous generation. Uniform crossover is used, where each bit has equal chance of being selected from each parent. Mutation is incorporated to alter the overstrength factor of a select number of anchors ± 0.1, as long as it stays within the range of 1–2. Algorithm parameter values were tuned empirically, and are given in Table 2. The algorithm is considered converged once the same configuration has been the fittest in the population for 100 consecutive generations. The algorithm stops once converged or if 5000 generations elapse, whichever comes first.

Additionally, it was discovered that seeding the initial population resulted in large increases in efficiency with negligible reductions in population diversity. The selection of initial seeds was also determined empirically. 40% of the initial population is seeded with turbine configurations expected to perform well. This set includes configurations considered to be good (though unlikely optimal) solutions to act as starting points to reduce computation time for the algorithm. The seeded configuration selections are shown in Table 3. Each seeded configuration has a uniform

Table 2 GA parameters of the optimization algorithm used in this work

Parameter	Value
Population size	100
Crossover percentage	70%
Cloning percentage	10%
Kill percentage	20%
Percentage of offspring mutated	10%
Bit mutation rate	10%

Table 3 Details of the 40 initial seeds used in the optimization algorithm

Anchors selected	Image	OSFs	Anchors Selected	Image	OSFs
All anchors	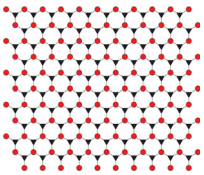	1.05, 1.10, 1.15, 1.20	Southern half of anchors	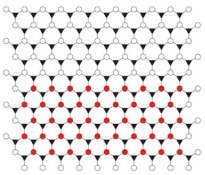	1.10, 1.20, 1.30, 1.40
Shared anchors in short columns	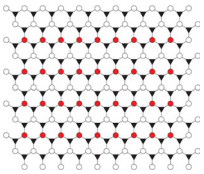	1.10, 1.20, 1.30, 1.40	Shared anchors in long columns	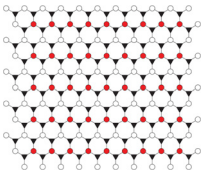	1.10, 1.20, 1.30, 1.40
Southern row of shared anchors	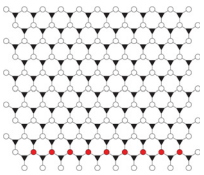	1.25, 1.50, 1.75, 2.00	Center three anchor rows	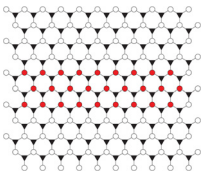	1.10, 1.20, 1.30, 1.40
Outer box of shared anchors	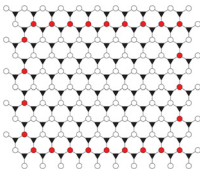	1.25, 1.50, 1.75, 2.00	All anchors with three connected lines	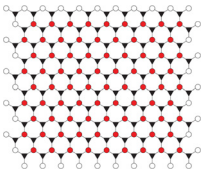	1.05, 1.10, 1.15, 1.20
All even numbered anchors	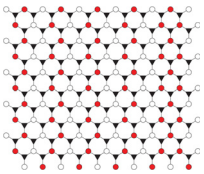	1.05, 1.10, 1.15, 1.20	All odd numbered anchors	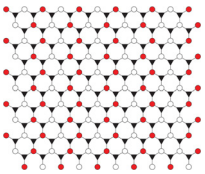	1.05, 1.10, 1.15, 1.20

Graphics in table are adapted from Ref. [14].

overstrength factor throughout all the overstrengthened anchors in the farm, though four overstrength factors were tested per combination of anchors (i.e., each row in Table 3 corresponds to four configurations, each with its own uniform overstrength factor).

The remainder of the initial population is composed of random configurations, as is typical for a GA. However, this set of the population is split: two-thirds of the random configurations have a uniform overstrength factor but random overstrengthened anchor selections, and one-third have both random overstrengthened anchor and overstrength factor selections. This was done because a decrease in computation time to convergence was found by adding the uniform overstrength factor individuals without significantly affected population diversity.

The fitness function used in the algorithm is given in Eq. (1). The fitness of an individual is equal to the cost difference between it and the worst surviving individual divided by the standard deviation of the costs of all surviving individuals

$$F_i = \frac{|C_i - C_{\text{last}}|}{\sigma_{\text{gen}}} \tag{1}$$

3.2 Bayesian Optimization. Bayesian optimization is commonly used in optimization problems where the objective function is largely unknown and expensive to evaluate. A prior probability distribution is generated from the objective function, with evaluation points probabilistically sampled. A posterior distribution is created after analyzing the results of the evaluations, forming an acquisition function that determines where the next evaluation points should be.

Incorporating elements of Bayesian optimization proved useful in this optimization algorithm since its methods are inherently tolerant to stochastic function evaluations. For this hybrid algorithm, the lognormal distribution of anchor and mooring line demands discussed in Sec. 2 function as the Bayesian prior, and the GA cloning, crossover, and mutation discussed in Sec. 3.1 act as the acquisition function.

Functionally, this means that the number of evaluation simulations for a configuration is dependent on its fitness, with fitter individuals being evaluated more times than less fit individuals. For the initial population, each configuration is simulated 3000 times, as this was the point at which good individuals could reliably be separated from mediocre and poor individuals (see Fig. 4). The algorithm stores an archive of all configurations, the total number of simulations ran for each configuration, and the average cost across all simulations for each configuration. For all subsequent generations, the algorithm queries the archive after the population is generated to identify which configurations already exist in the archive. The algorithm then retrieves the archived cost, simulates the configuration an additional 1500 times, calculates an updated average cost, and restores the new values to the archive. Configurations not stored in the database are simulated 3000 times and subsequently stored, as was done with the initial population. This addition is shown in Fig. 3 above.

With this process, the best configurations are simulated an increasingly large number of times, gradually reducing the variance in its cost. Meanwhile, poor configurations are only

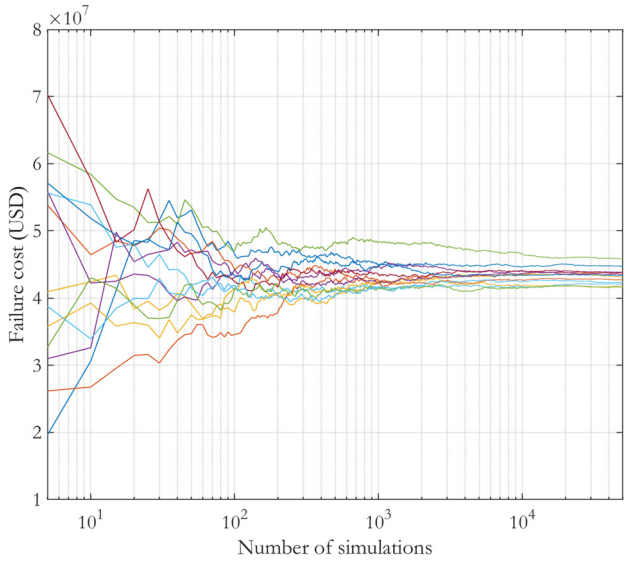

Fig. 4 Reduction in cost variance due to additional simulations. Adapted from Ref. [14].

simulated enough times to confirm they are not evaluating well before dying out via the GA selection process. In a simulation of 25 random configurations (sample data included in Fig. 4), configurations could be reliably ranked after 150,000 total simulations, which determined the 100 generation threshold to decide convergence. Therefore, by convergence, the optimal cost should have very low error associated with its cost.

4 Cost Model

The optimization algorithm uses a cost model to evaluate (1) the added capital costs due to overstrengthening the selected anchors, and (2) the added costs from performing need-based maintenance to repair the failures from loss of stationkeeping.

The overall equation for the added cost of a configuration is

$$C_i = \frac{\sum_{1}^{n_{\text{sims}}} C_{\text{failure}}}{n_{\text{sims}}} + C_{\text{osf}} \tag{2}$$

The failure cost is averaged from all the evaluations as discussed above in Sec. 3.2. The failure cost for each simulation is based on the total number of turbines with at least one mooring line or anchor failure, at which point stationkeeping is lost. The cost components consist of the likeliest perceived costs that could occur in the event of a floating wind turbine losing stationkeeping. The total failure cost for a given simulation is given as

$$C_{\text{failure}} = C_{\text{moor}} + C_{\text{elec}} + C_{\text{turb}} + C_{\text{downtime}} \tag{3}$$

Each component of Eq. (3) is detailed below in Secs. 4.1–4.4.

The overstrength factor cost is the *additional* cost of manufacturing the overstrengthened anchors compared to the normal strength anchors. Details of the overstrength factor cost are detailed below in Sec. 4.5.

It is worth noting that this cost model is not meant to be comprehensive. The addition of the cost model here is used as a tool to demonstrate the tradeoffs between cost and reliability in the optimization algorithm. However, cost accuracy was approached with care, and values are derived from existing literature when possible. A cost sensitivity analysis is also performed to examine differences in algorithm behavior for different cost profiles (see Sec. 4.6).

4.1 Mooring System Repair. As no shared anchoring system has ever been tested, various assumptions had to be made regarding the anchor and line replacement process:

- The entire anchor is assumed to be replaced regardless of failure mode. On suction caissons, the padeye (the connection point on the anchor for the mooring line) is below the seabed for an installed turbine. Therefore, even if partial removal and reinstallation of a suction caisson were a repair option, it would be logistically challenging (particularly for a shared anchor), and a complete reinstallation is likely less expensive [19]. While the evaluation in this work only considers anchor failures from soil degradation, this rule would hold if torsional failures on the padeye were considered, as these have also been reported to be likely during hurricanes [20].
- Similarly, in the event where a mooring line fails but its anchor does not, the entire anchor is still replaced.
- The reinstallation of failed anchors begins after all formerly connected turbines are towed to port.
- One anchor handling tug supply (AHTS) vessel with subsea equipment is used to reinstall an anchor. While AHTS vessels often drop anchors directly from the vessel without subsea equipment due to cost savings, precision in install location is vital due to the coupled nature of shared anchors, so subsea equipment must be used.
- Three AHTS vessels, one per turbine, are used to reconnect the mooring lines to the platform fairleads.
- A complete anchor reinstallation is assumed to take 14 h total. Myhr et al. [21] used a 12-hour installation time for single-line suction caissons, and one additional hour is added per extra mooring line due to vessel maneuvering and handling complexities from connecting multiple lines to one anchor.

The costs for different items considered are included in Table 4. All monetary values derived from literature are converted to 2020 U.S. dollars. The anchor material cost is assumed to be directly proportional to the anchor mass, which depends on the ultimate holding capacity. The required anchor mass for a given anchor strength (factoring in the overstrength factor of the anchor) is calculated from its density and volume; in turn, the anchor volume is calculated using the design equations for pile anchors given by the American Bureau of Shipping [22]

$$L, D, T = c * S_{ult}^{d} \tag{4}$$

where c and d are (1.1161, 0.3095, and 2.0580) and (0.3442, 0.2798, and 0.2803) for (L, D, T), respectively, using the

Table 4 Details of mooring system repair

Item	Failure Cost	Notes	Citation
Mooring line material cost	$208,750 per line	$250/m in 200 m water depth	[21]
Anchor material cost	Variable	See text	[21]
Anchor decommissioning cost	$903,828 per anchor		[23]
Anchor disposal cost	$495,887	Covers all failed anchors	[23]
Labor and vessel costs	$343,720 per anchor	Method 1 from Castro-Santos et al.	[23]
Vessel transit time	3 hours	50 NM at 16 knots	[24]
On-site repair time	14 hours	2 hours more than citation—see text	[24]

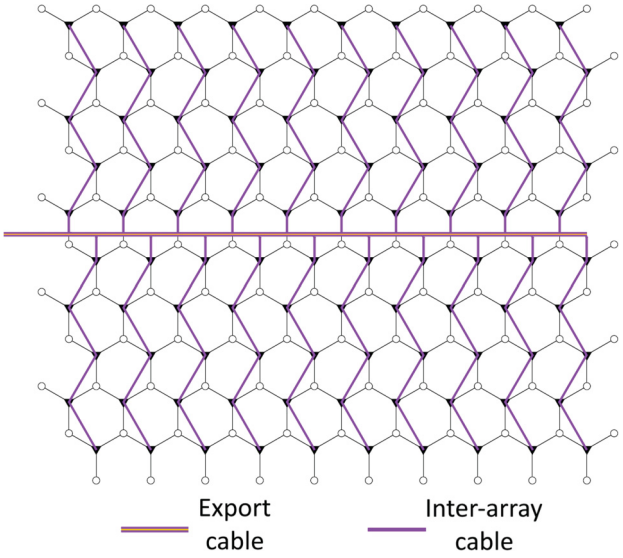

Fig. 5 Schematic of electric cable layout in the analyzed wind farm. Adapted from Ref. [14].

American Bureau of Shipping (ABS) constants for suction piles in very soft clay. A material cost of the anchor steel is set at \$12,300/ton, as used in Myhr et al. [21], and the density of steel is assumed to be 7,850 kg/m^3.

4.2 Electrical Repair. The drift and rotation of a platform caused by even partial loss of stationkeeping will almost certainly result in damage or failure of the interarray cable for the turbine in question. Therefore, every turbine in the simulation that suffers at least one component failure in its mooring system is assumed to require electrical repair.

The layout of the electrical cabling for the wind farm is shown in Fig. 5, which uses a convention radial collection system, similar to what is used in the 100 turbine wind farm analyzed by Bjerkseter and Ågotnes [24]. Considering the location of the farm in the Gulf of Maine, the export cable continues east to the coast to connect with land-based transmission lines. The interarray cables are assumed to be connected serially between turbines without redundancy. As a result, the electrical failure of one turbine results in the loss of power to all downstream turbines, even if those turbines maintain stationkeeping. This impacts the downtime power losses substantially, as explored in Sec. 4.4.

The electrical repair begins after the anchor system and turbine repairs are complete and all turbines have been reinstalled in the farm. The entire cable length for a particular unmoored turbine is assumed to be removed and replaced with a cable laying vessel. The costs and other relevant information associated with interarray cable repairs are detailed in Table 5.

4.3 Turbine Repair. Virtually, no literature exists regarding the expected damage to floating offshore wind turbines due to loss of stationkeeping. While the damage to an unmoored floating wind turbine in the midst of a 500-year storm has the potential to be catastrophic, the probability of these failures, which failure modes to consider, and isolating the damages that would *not* occur absent loss of stationkeeping is impossible to approximate given the current state of research. Due to this, assumptions regarding turbine repairs from loss of stationkeeping are kept generalized and conservative.

The cost model assumes all turbines that lose stationkeeping are towed to shore by an AHTS as soon as it is safe to do so to undergo inspections, prior to the mooring system repairs. Each turbine is assumed to be quayside for one week to undergo major repairs to the gearbox, hub, blades, and yaw system, as specified by Carroll et al. [26]. The mooring system repairs are assumed to occur while the turbines are quayside, and the turbines are towed back to the farm and reinstalled at the end of the week. Costs associated with turbine repair are detailed in Table 6.

4.4 Costs From Lost Power. Costs of lost production must be considered for turbines that go offline due to electrical failures. As with the other failure cost components, only downtime resulting directly from a loss of stationkeeping is considered in this research.

Levelized cost of energy is used to translate lost power production into a cost-equivalent to add to this cost model. An LCOE of \$132/MWh is used as given by Stehly and Beiter [4]—while the LCOE at the point in the future when a floating wind farm of this scale is feasible will likely be far lower, estimating that extends beyond the scope of this work. The total cost-equivalent from lost power is

$$C_{\text{downtime}} = \text{LCOE} * P * k_{\text{cf}} * n_{\text{tpr}} * n_{\text{rows}} * t_{\text{repair}} \tag{5}$$

where k_{cf} is assumed to be 0.44. The total repair time for each failed site is

Table 5 Details of electrical system repair

Item	Failure cost	Notes	Citation
Interarray cable material cost	\$805,916 per turbine	\$481/m	[25]
Replacement cable length	1675.5 m	Based on farm geometry	
Vessel and labor costs	\$258,027 per turbine	\$154/m	[25]
Cable laying rate	400 m per day		

Table 6 Details of turbine system repairs

Item	Failure cost	Notes	Citation
Turbine tow vessel cost	\$727,942 per turbine		[24]
Turbine quayside time	1 week		
Gearbox repair material costs	\$3000 per turbine	Major repair from Carroll et al.	[26]
Hub repair material costs	\$3000 per turbine	Major repair from Carroll et al.	[26]
Blade repair material costs	\$1800 per turbine	Major repair from Carroll et al.	[26]
Yaw system repair material costs	\$3600 per turbine	Major repair from Carroll et al.	[26]
Quayside labor costs	\$109,985 per turbine	From annual labor crew costs	[21]

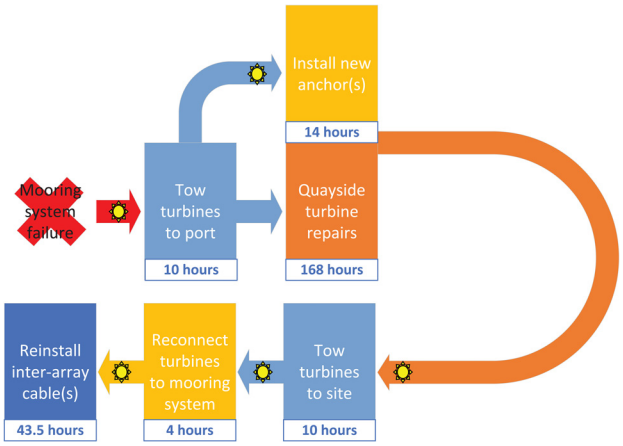

Fig. 6 Repair process following a mooring system failure. The sun symbols on arrows indicate a weather window must open before the next action can be performed. Adapted from Ref. [14].

$$t_{\text{repair}} = t_{\text{weather}} + t_{\text{labor}} \tag{6}$$

The total repair process, and the time required for each step, is summarized in Fig. 6.

The maintenance delays due to poor weather for offshore wind installations are far higher than for onshore turbines, and floating installations are expected to have even longer delays than fixed-bottom offshore wind due to the increased travel times and generally more severe metocean climates further from shore [6]. For determining the delay time in waiting for a weather window for this particular site, 37 years of metocean data was collected from National Oceanic and Atmospheric Administration (NOAA) Station 44005, available from the National Buoy Data Center [27], to determine the frequency and length of weather windows. Weather window thresholds were set at 2 meters significant wave height, from the value given for AHTS vessels by Brons-Illing [28], and a maximum sea level wind speed of 12 m/s, as per Dowell et al. [29].

For every 12 h of total repair time (excluding the time the turbine is quayside), a random sample is used to determine whether a 12 h weather window occurs, in which case the repairs can proceed without delay. If the random sample falls outside the weather window probability, the delay is determined by randomly sampling the downtime lengths from the NOAA data. This process is repeated until all repairs have been completed.

4.5 Capital Costs of Overstrengthening Anchors. The capital costs for overstrengthening the specified anchors in a particular configuration are computed as

$$C_{\text{osf}} = \sum_{i=1}^{n_{\text{os}}} C_i - C_{\text{unstr}} \tag{7}$$

The method of finding the costs of the overstrengthened anchors and an unstrengthened anchor are identical to the method discussed in Sec. 4.1 using the ABS equation.

4.6 Cost Sensitivity Analysis. Despite the floating offshore wind cost estimates made in previous works and cost parallels that can be made with onshore and fixed-bottom offshore wind, the cost model used here is highly speculative. Virtually, no publicly available data exists for operations and maintenance costs for floating wind turbines due to the nascence of the industry. Furthermore, these values are difficult to even predict due to fluctuations in the cost of steel, duration of repairs, and vessel costs and availability. These uncertainties are exacerbated in the U.S., which does not have an established supply chain for fixed-bottom offshore wind (let al.one floating offshore wind), and is further complicated by restrictions on the use of foreign vessels in American waters by the Jones Act [30].

Because of these reasons, a cost sensitivity analysis is performed in this work to evaluate the differences in tradeoffs between reliability and cost for different cost profiles. The profiles selected are meant to evaluate the elements of the cost model thought to have the highest uncertainty in cost, with the multiplier selected so profiles B and C have roughly the same cost when tested with an optimal configuration from profile A. The three cost profiles are considered in this work:

- Profile A: The baseline cost model. All costs specified throughout Sec. 4 are unchanged.
- Profile B: Costs associated with mooring system repairs are increased by a factor of 3. This represents cost uncertainties related to cost of steel for anchors, vessel costs, and complications involving working with shared anchors.
- Profile C: Costs and downtime associated with turbine quayside repairs are increased by a factor of 5. This represents uncertainties regarding the severity of turbine damage caused by loss of stationkeeping during a severe storm.

5 Results and Discussion

For all profiles, the algorithm stopped after reaching the 5000 generation limit. However, upon analyzing the results, it appears that a minimal cost is consistently achieved by around generation 2000, but there are many combinations of overstrength factors that achieve the minimum cost. This is not surprising, given the size and symmetry of the wind farm. Additionally, all of the optimal configurations show very similar behavior, enabling us to draw valuable conclusions about the mooring system design and reliability. Statistical information about the optimal costs is included in Table 7.

The configuration with the lowest cost would change every few generations due to the continuously updating costs for each configuration, preventing the algorithm from meeting the standard convergence criterion. While it is possible that this algorithm would eventually find a single optimal solution, it would likely take a prohibitively long time and would provide little new information or practical benefit than what is achieved here. As a test, Profile A was simulated for an additional 2000 generations using a population entirely of optimal anchor configurations from earlier testing, with a much higher cloning percentage to encourage rapid reduction in cost uncertainty. Despite this, there was less than a 5% reduction in standard deviation, with no apparent convergence to a single optimal configuration.

5.1 Anchor and Overstrength Factor Selection. Sample configurations of different optimal selections are given in Table 8. These do not represent all of the optimal configurations for each profile, merely a subset that is representative of the diversity of patterns seen in the optimal set as a whole. Notably, despite the

Table 7 Added cost results of the optimization algorithm

Cost profile	Mean optimal cost	Standard deviation	Mean absolute percentage error
A	$12,794,221	$53,397	0.32%
B	$14,795,386	$53,402	0.29%
C	$14,327,646	$57,660	0.32%

Table 8 Sample results of the optimization algorithm

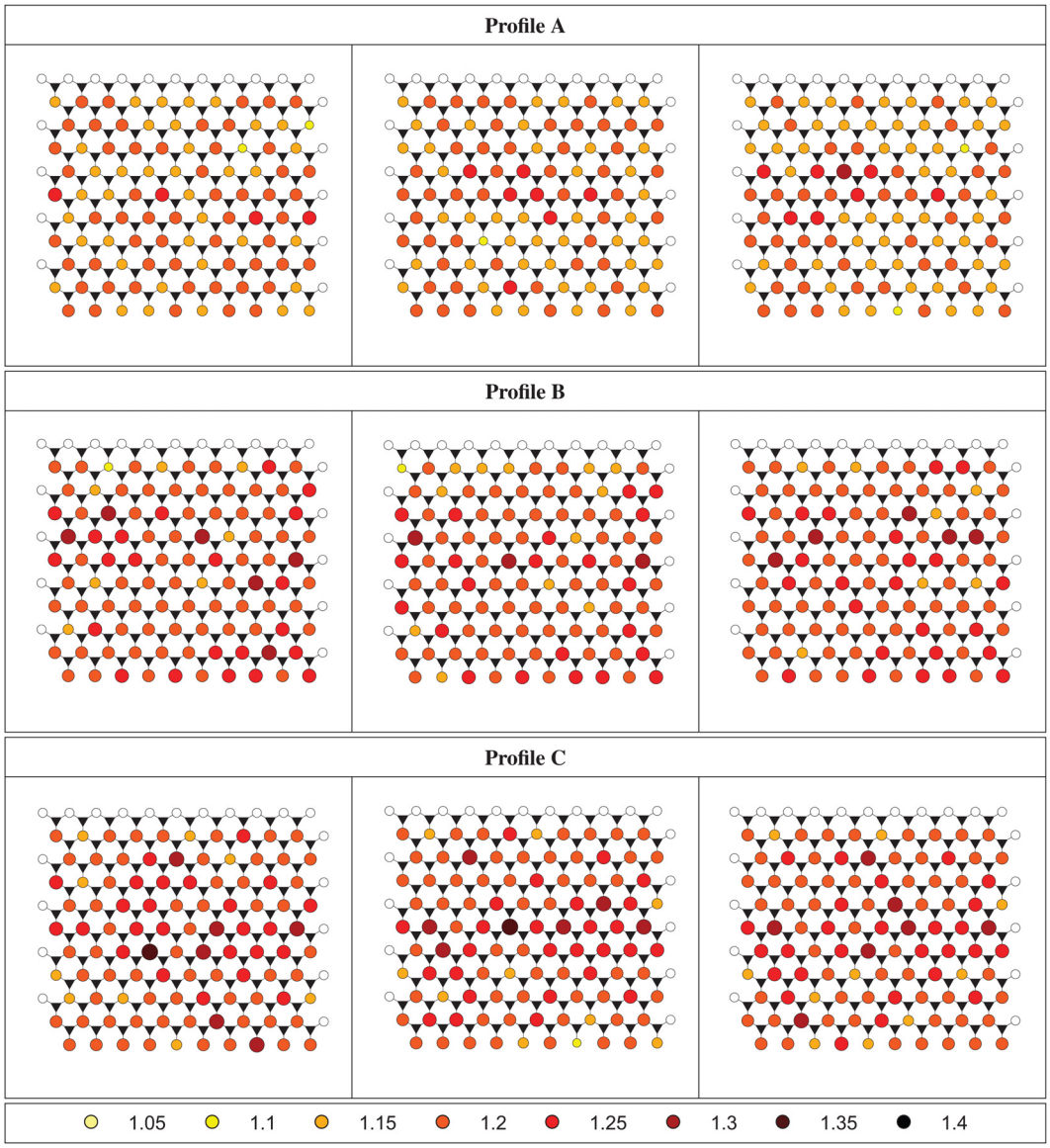

Anchor color indicates its overstrength factor. Graphics in table are adapted from Ref. [14].

similarity in patterns between the optimal configurations, specific patterns of anchor *numbers* rarely appear. Due to this, it is probable that the minimum costs here approach a global optimum, as it suggests that these configurations were discovered independently of one another by the algorithm.

All optimal configurations for all profiles overstrengthen every anchor in the wind farm except for the unshared anchors on the eastern, western, and northern edges of the farm. Overstrength factors are kept relatively low, with no factor ever exceeding 1.35. The unshared anchors on the southern edge of the wind farm are likely overstrengthened due to the wind and wave directions in the evaluation coming from the south, making this row of anchors (and the southernmost anchor on each turbine in general) suffer much higher failure rates than the other unshared anchors.

Profile C has the highest average overstrength factor, and Profile A has the lowest. The latter is expected, considering the lower failure costs make the risk of component failure less severe. Profile C having a higher average overstrength factor than Profile B is somewhat unexpected, considering the similar costs of the two profiles. It is likely that the failure of a single turbine in profile C is far more severe than in Profile B since the costs from lost power are much higher, particularly if a single component failure causes the loss of power to several turbines. Profile C also shows markedly less pattern consistency in overstrength factor locations. This may be due to the amplifications of downtime costs making the impact of the variance in determining weather delays much greater, increasing the uncertainty in the optimization problem.

Noticeable patterns emerge when comparing the overstrength factors north to south. All three profiles show the center rows consistently have the highest average overstrength factor in the farm. This is likely due to the high impact of an electrical failure of turbines near the middle rows, as the serial connection of interarray cables can cause up to five turbines to lose power due to a single component failure. Profile B also shows a concentration of higher overstrength factors at the southern end of the farm compared to the other two profiles. This is perhaps due to the risk of cascading failures propagating from the south, as the southernmost anchor of each turbine is at the highest risk of failure as discussed above. Due to the amplified mooring system repair costs in profile B, it would make sense to reduce mooring system failure more than the

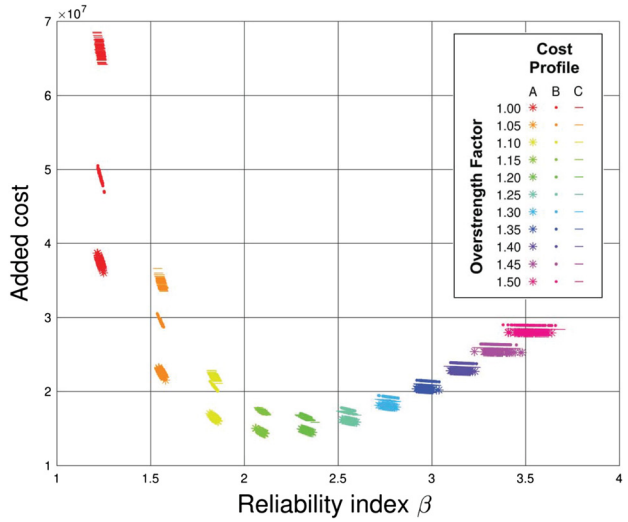

Fig. 7 Comparison of system reliability evaluation and added cost evaluation for a farm with uniformly strengthened anchors. Adapted from Ref. [14].

other profiles. The north of the farm sees the lowest average overstrength factors for similar reasons, though this is less pronounced in profile C.

No clear patterns emerge when comparing overstrength factors east to west. Spreading out the anchors with higher overstrength factors seems to occur more often than not, though there are many exceptions to this (some included in Table 8). Still, spreading out the highest strength anchors is logical since it reduces the risk of both south-to-north cascading failures and severe electrical losses. The lack of patterns east to west is not surprising, as both the evaluated storm conditions and interarray connections propagate north to south in this work.

5.2 Added Cost Versus Reliability. Based on the results of the array optimization, an additional test was performed to identify a more detailed interaction between system reliability (as calculated by the system reliability evaluation discussed in Sec. 2) and added cost across the different cost profiles. A configuration was created for each profile where all the anchors selected in Sec. 5.1 are overstrengthened to a uniform factor ranging from 1.05 to 1.5. A configuration with no overstrengthening (i.e., an overstrength factor of 1) was also tested. Each configuration is evaluated 100 times, with each evaluation consisting of 3,000 simulations.

The results of this test are shown in Fig. 7. As expected from the optimization results, added costs minimize with fairly low overstrength factors, at 1.15 for profile A and at 1.2 for profiles B and C, before slowly beginning to increase despite improved system reliability. This indicates a risk tradeoff still exists between cost and reliability for all three profiles, as the minimum cost occurs at $\beta \approx 2.25$, equating to about a 1.25% probability of turbine mooring system failure.

Profile C has drastically higher costs than Profile B for the farms with the lowest anchor strength, but these costs converge around an overstrength factor of 1.1, with profile B eventually becoming slightly more expensive than C for overstrength factors 1.25 and above. This suggests that decreasing the overall number of failures reduces costs for Profile C much more drastically than for profile B. This could point to the importance of further research into expected floating wind turbine damage in survival load cases, as farm design related to this could provide huge maintenance cost savings for relatively minor capital cost increases.

Notably, the minimum costs are also around $3 million higher than the optimized results found, suggesting significant cost savings by optimizing strength selection. However, the cost model in this work does not consider the additional manufacturing costs associated with the need of producing multiple anchor sizes. The cost of this may be more impactful than any cost savings from having multiple anchor strengths with precise placement locations. Ultimately, this is difficult to conclude one way or another given the uncertainties still surrounding costs and logistics in large floating offshore wind farm installations, whether included in the cost model or not.

6 Conclusions and Future Work

By the end of the 2020s, floating offshore wind will likely make a significant contribution to the renewable energy portfolio of the United States. At the present, however, the substantial costs, risks, and uncertainties associated with floating offshore wind prevent it from being commercially viable. The main objective of this work is to provide an optimization algorithm to analyze the tradeoffs between system reliability and added capital costs. A large wind farm using a shared mooring system is considered due to known shortfalls regarding its system reliability. Accounting for cost-normalized system reliability can reduce risks and uncertainties that currently exist with both the shared anchoring concept and, more broadly, the development of floating offshore wind farms.

Results reveal that the reduced system reliability in the shared mooring system is best remedied by increasing the strength of all shared anchors and windward unshared anchors. The optimization study identifies many similar configurations with added costs very close to the global minimum. Anchors supporting turbines nearest the export cable have their strength increased the most across all cost profiles. When the costs of mooring system repair are amplified, the strength of windward anchors is increased nearly as much as the anchors near the export cables. The lowest cost solutions retain about a 1.25% probability of failure due to loss of station-keeping, indicating improving reliability above this point is not worth further capital cost investment into the mooring system.

Results also indicate that system reliability is particularly sensitive to changes in turbine-related repair costs. Based on this, refinement of expected failure modes for floating offshore wind turbines under extreme loads could drastically improve the precision of computational simulations similar to the one performed in this work. Ultimately, this could have major positive impacts on floating wind farm system design, and is recommended by the authors as an area of future research focus.

While the optimization problem here could be answered by merely approaching a global optima, this work demonstrates the challenge of solving optimization problems with high uncertainty, even when consciously addressing it using Bayesian methods. The high degree of uncertainty in floating offshore wind technology would likely have prohibitively high computation time for more complex nondifferentiable optimization problems, such as detailed continuous field layout optimizations. Creating concrete decisions regarding supply chain logistics and maintenance strategies for the American offshore wind sector would reduce systematic uncertainty in these optimization problems, which could ultimately provide great benefit to system optimization work in the research community.

Imminent future work will entail applying this optimization algorithm to an equivalent floating wind farm with a traditional, single line mooring system. This could provide insight into whether the costs of an optimized farm with shared anchors provides financial benefit over traditional anchors despite the difference in system reliability. Other topics of future work include using a more efficient sampling technique in the evaluation function to further reduce convergence time, and expanding the optimization algorithm beyond the specific demonstration case studied here. Adding elements such as altered metocean conditions, different mooring system dispositions, and different floating platform models are of particular interest, as these generalize the

algorithm for use in other areas of research in the floating offshore wind community.

Nomenclature

C_{downtime} = costs associated with lost power generation due to repair downtime
C_{elec} = costs associated with electrical system repairs
C_{failure} = total maintenance costs associated with the failure of a single wind turbine from loss of stationkeeping
C_i = total added costs for individual i
C_{last} = total added costs for the worst surviving individual in a population
C_{moor} = costs associated with mooring system repairs
C_{osf} = capital costs associating with manufacturing anchors with an overstrength factor greater than 1
C_{turb} = costs associated with turbine repairs
C_{unstr} = cost of an anchor with the nominal capacity (i.e., overstrength factor of 1)
FOWT = floating offshore wind turbine
GA = genetic algorithm
k_{cf} = turbine capacity factor
LCOE = levelized cost of energy
n_{rows} = number of inter-array cable strings with unmoored turbines
n_{sims} = number of Monte Carlo simulations in a single evaluation
n_{tpr} = average number of unmoored turbines per inter-array cable string, among the strings that experience 1 or more failures
OSF = overstrength factor
P = turbine power rating
t_{labor} = total time spent performing repair procedures
t_{weather} = total time spent waiting for repair weather windows
β = reliability index
σ_{gen} = standard deviation of a surviving population

Appendix: Availability of Material

The MATLAB code used to generate the results in this work is openly available via the REL-OPT software package [10]. The most recent version of REL-OPT can be found at its GitHub repository.[3] All figures and graphics used in this work are also openly available under the CC-BY license [14].

References

[1] Musial, W., Beiter, P., Spitsen, P., Nunemaker, J., and Gevorgian, V., 2019, "2018 Offshore Wind Technologies Market Report," U.S. Department of Energy, Oak Ridge, TN, Report No. NREL/TP-5000-74278.
[2] Nagle, M., 2020, *Diamond Offshore Wind, RWE Renewables Join the University of Maine to Lead Development of Maine Floating Offshore Wind Demonstration Project*, UMaine News - University of Maine, Section: Advanced Materials for Infrastructure and Energy, Orono, ME.
[3] Hill, J. S., 2018, "Hywind Scotland, World's First Floating Wind Farm, Performing Better Than Expected," CleanTechnica, accessed July 22, 2021, https://cleantechnica.com/2018/02/16/hywind-scotland-worlds-first-floating-wind-farm-performing-better-expected/
[4] Stehly, T., and Beiter, P., 2019, "2018 Cost of Wind Energy Review," Renewable Energy, p. 71.
[5] Musial, W., and Ram, B., 2010, "Large-Scale Offshore Wind Power in the United States: Assessment of Opportunities and Barriers," National Renewable Energy Laboratory, Golden, CO, Report No. NREL/TP-500-40745.
[6] Clark, C. E., and DuPont, B., 2018, "Reliability-Based Design Optimization in Offshore Renewable Energy Systems," Renewable Sustainable Energy Rev., **97**, pp. 390–400.
[7] Fontana, C. M., Arwade, S. R., DeGroot, D. J., Myers, A. T., Landon, M., and Aubeny, C., 2016, "Efficient Multiline Anchor Systems for Floating Offshore Wind Turbines," ASME 2016 35th International Conference on Ocean, Offshore and Arctic Engineering, Busan, South Korea, June 19–24.
[8] Fontana, C. M., Hallowell, S. T., Arwade, S. R., DeGroot, D. J., Landon, M. E., Aubeny, C. P., Diaz, B., Myers, A. T., and Ozmutlu, S., 2018, "Multiline Anchor Force Dynamics in Floating Offshore Wind Turbines," Wind Energy, **21**(11), pp. 1177–1190.
[9] Hallowell, S. T., Arwade, S. R., Fontana, C. M., DeGroot, D. J., Aubeny, C. P., Diaz, B. D., Myers, A. T., and Landon, M. E., 2018, "System Reliability of Floating Offshore Wind Farms With Multiline Anchors," Ocean Eng., **160**, pp. 94–104.
[10] Devin, M. C., and Hallowell, S. T., 2020, "Rel-Opt," accessed July 22, 2021, https://doi.org/10.5281/zenodo.4059098.
[11] Robertson, A., Jonkman, J., Masciola, M., Song, H., Goupee, A., Coulling, A., and Luan, C., 2014, "Definition of the Semisubmersible Floating System for Phase II of OC4," National Renewable Energy Laboratory, Golden, CO, Report No. NREL/TP-5000-60601, 1155123.
[12] Jonkman, J., Butterfield, S., Musial, W., and Scott, G., 2009, "Definition of a 5-MW Reference Wind Turbine for Offshore System Development," National Renewable Energy Laboratory, Golden, CO, Report No. NREL/TP-500-38060, 947422.
[13] González-Longatt, F., Wall, P., and Terzija, V., 2012, "Wake Effect in Wind Farm Performance: Steady-State and Dynamic Behavior," Renewable Energy, **39**(1), pp. 329–338.
[14] Devin, M., 2019, "Optimizing Strength of Shared Anchors in an Array of Floating Offshore Wind Turbines," Honors College Thesis, Mechanical Engineering, Oregon State University, Oregon.
[15] Jonkman, J. M., 2013, "The New Modularization Framework for the FAST Wind Turbine CAE Tool," AIAA Paper No. 2013-0202.
[16] Viselli, A. M., Goupee, A. J., Dagher, H. J., and Allen, C. K., 2016, "Design and Model Confirmation of the Intermediate Scale Floating Wind Turbine Subjected to Its Extreme Design Conditions Offshore Marine," Wind Energy, **19**(6), pp. 1161–1177.
[17] Choi, Y. J., 2007, "Reliability Assessment of Foundations for Offshore Mooring Systems Under Extreme Environments," Ph.D. dissertation, The University of Texas at Austin, Austin, TX.
[18] Painton, L., and Campbell, J., 1995, "Genetic Algorithms in Optimization of System Reliability," IEEE Trans. Reliab., **44**(2), pp. 172–178.
[19] Houlsby, G. T., and Byrne, B. W., 2000, "Suction Caisson Foundations for Offshore Wind Turbines and Anemometer Masts," Wind Eng., **24**(4), pp. 249–255.
[20] Ward, E. G., Zhang, J., Kim, M. H., Aubeny, C., Mercier, R. S., and Gilbert, R. B., 2008, "No Modus Adrift: Final Project Report," Texas A&M University, College Station, TX, Report No. 1435-01-04-CA-35515.
[21] Myhr, A., Bjerkseter, C., Ågotnes, A., and Nygaard, T. A., 2014, "Levelised Cost of Energy for Offshore Floating Wind Turbines in a Life Cycle Perspective," Renewable Energy, **66**, pp. 714–728.
[22] ABS, 2013, "Offshore Anchor Data for Preliminary Design of Anchors of Floating Offshore Wind Turbines," American Bureau of Shipping, Houston, TX.
[23] Castro Santos, L., Ferreño González, S., and Diaz Casas, V., 2013, "Methodology to Calculate Mooring and Anchoring Costs of Floating Offshore Wind devices," International Conference on Renewable Energy and Power Quality 11, pp. 268–272.
[24] Bjerkseter, C., and Ågotnes, A., 2013, "Levelised Costs of Energy for Offshore Floating Wind Turbine Concepts," Master's thesis, Norwegian University of Life Sciences, Ås, Norway.
[25] Gonzalez-Rodriguez, A. G., 2017, "Review of Offshore Wind Farm Cost Components," Energy Sustainable Dev., **37**, pp. 10–19.
[26] Carroll, J., McDonald, A., and McMillan, D., 2016, "Failure Rate, Repair Time and Unscheduled O&M Cost Analysis of Offshore Wind Turbines: Reliability and Maintenance of Offshore Wind Turbines," Wind Energy, **19**(6), pp. 1107–1119.
[27] NOAA, 2020, "National Data Buoy Center," https://www.ndbc.noaa.gov/
[28] Brons-Illing, C., 2015, "Analysis of Operation and Maintenance Strategies for Floating Offshore Wind Farms.pdf," Master's thesis, University of Stavanger, Stavanger, Norway.
[29] Dowell, J., Walls, L., Zitrou, A., and Infield, D. 2013, *Analysis of Wind and Wave Data to Assess Maintenance Access to Offshore Wind Farms*, 22nd ESREL Conference 2013, Amsterdam, The Netherlands, Sep. 29–Oct. 2, pp. 743–750.
[30] Papavizas, C., 2011, "Clarifying the Jones Act for Offshore Wind," North Am. Wind Power, p. 2.

[3] https://github.com/michaelcdevin/Rel-Opt